

Synthesis, characterization and biocompatibility studies of zinc oxide (ZnO) nanorods for biomedical application

R. Gopikrishnan¹, K. Zhang², P. Ravichandran¹, S. Baluchamy¹, V. Ramesh¹, S. Biradar¹, P. Ramesh³, J. Pradhan², J. C. Hall¹, A. K. Pradhan² and G. T. Ramesh^{1,*}

Nanoparticles are increasingly being recognized for their potential utility in biological applications including nanomedicine. Here, we have synthesized zinc oxide (ZnO) nanorods using zinc acetate and hexamethylenetetramine as precursors followed by characterizing using X-ray diffraction, fourier transform infrared spectroscopy, scanning electron microscopy and transmission electron microscopy. The growth of synthesized zinc oxide nanorods was found to be very close to its hexagonal nature, which is confirmed by X-ray diffraction. The nanorod was grown perpendicular to the long-axis and grew along the [001] direction, which is the nature of ZnO growth. The morphology of synthesized ZnO nanorods from the individual crystalline nucleus was confirmed by scanning and transmission electron microscopy. The length of the nanorod was estimated to be around 21 nm in diameter and 50 nm in length. Our toxicology studies showed that synthesized ZnO nanorods exposure on hela cells has no significant induction of oxidative stress or cell death even in higher concentration (10 µg/ml). The results suggest that ZnO nanorods might be a safer nanomaterial for biological applications.

Keywords: Zinc oxide [ZnO]; Nanorods; XRD; SEM & TEM; Cytotoxicity

Citation: R. Gopikrishnan, K. Zhang, P. Ravichandran, S. Baluchamy, V. Ramesh, S. Biradar, P. Ramesh, J. Pradhan, J. C. Hall, A. K. Pradhan and G. T. Ramesh, "Synthesis, characterization and biocompatibility studies of zinc oxide (ZnO) nanorods for biomedical application", Nano-Micro Lett. 2, 31-36 (2010). [doi: 10.5101/nml.v2i1.p31-36](https://doi.org/10.5101/nml.v2i1.p31-36)

Nanotechnology has extraordinary potential to change our lives by improving existing products and enabling new ones. It facilitates the development of new materials in the 1~100 nm range, comparable to the size range of biological molecules and structures [1]. Nanomaterials are very attractive materials for the manipulation, sensing and detection of biological structures and systems [2]. The principal factors which make nanomaterials different from their bulk counterparts include an increase in their relative surface area and quantum effects, which affect their physical and chemical properties [2]. This is due to the large surface area-to-volume ratio of nanoparticles, which increases surface free energy to a point that is comparable to their lattice energy. For example, a particle of 30 nm size has 5% of its atoms

on its surface compared to 50% of the atoms on the surface of a 3 nm particle [3]. The altered properties of nanomaterials, and their size similarity to naturally occurring cell structures, will allow them to interact readily with bio molecules and potentially affect the cellular responses in a dynamic and selective manner. Materials that exploit these characteristics are becoming increasingly attractive for use in novel biomedical applications.

Nano structured materials exhibit unique properties related to their size, and are used in an array of applications such as optoelectronics, nano/microelectronics, sensors, transducers, cosmetics as well as medical applications such as biosensors, tissue engineering and drug delivery vehicles [4-6]. Although our understanding of the human body at nanometer scale has

¹ Molecular Toxicology Laboratory, Center for Biotechnology and Biomedical Sciences, Norfolk State University, 700 Park Avenue, Norfolk, VA, 23504, USA

² Center for Materials Research, Norfolk State University, 700 Park Avenue, Norfolk, VA 23504, USA

³ Health Science Academy, Bayside High School, Virginia Beach, 4960 Haygood Road, VA 23455, USA

*Corresponding author. Email: gtramesh@nsu.edu

improved tremendously, advances in therapeutic options for treating severe diseases, such as cancer and autoimmunity have lagged by comparison. In this regard, nanomedicine, which is the most important application of nanotechnology to medical problems, can offer new approaches.

Zinc oxide [ZnO] is a semiconductor material with various configurations, much richer than of any other known nanomaterial [7,8]. At nanoscale, it possesses unique electronic and optoelectronic properties and finds application as biosensors, sunscreens, as well as in medical applications like dental filling materials and wound healing [9]. Because of the indiscriminate use of ZnO nanoparticles, it is important to look at their biocompatibility with biological system. A recent study on ZnO reports that it induces much greater cytotoxicity than non-metal nanoparticles on primary mouse embryo fibroblast cells [10], and induces apoptosis in neural stem cell [11]. Published reports have shown that ZnO inhibits the seed germination and root growth [12]; exhibit antibacterial properties towards *Bacillus subtilis* and to a lesser extent to *Escherichia coli* [13]. Inhalation of ZnO compromises pulmonary function in pigs and causes pulmonary impairment and metal fume fever in humans [14,15]. Literature evidences showed that ZnO nanoparticles are the most toxic nanoparticle with the lowest LD50 value among the engineered metal oxide nanoparticles [16]. On the other hand, it was also reported that zinc oxide was not found to be cytotoxic to cultured human dermal fibroblasts [17]. In recent years, there has been an escalation in the development of techniques for synthesis of nanorods and subsequent surface functionalization. ZnO nanorods exhibit characteristic electronic, optical, and catalytic properties significantly different from other nano metals. Keeping in view of the unique properties and the extensive use of ZnO in many fields and also contradictory results on ZnO toxicity from both in-vitro and in-vivo studies, we report here to synthesize and characterize the ZnO nanorods on hela cells for its biocompatibility/toxicity.

Materials and methods

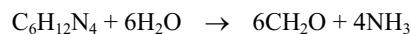
Materials

Zinc acetate anhydrous ($\text{Zn}(\text{O}_2\text{CCH}_3)_2$) and hexamethylenetetramine ($\text{C}_6\text{H}_{12}\text{N}_4$) were purchased from Alfa Aesar (MA, USA), dulbecco's modified magle medium (DMEM), phosphate buffered saline (PBS), fetal bovine serum (FBS), and hank's balanced salt solution (HBSS) were obtained from Atlanta Biologicals, Inc. (Atlanta, GA). RPMI-1640 medium, glutathione (GSH), 3-(4,5-dimethylthiazol-2-yl)-2,5-diphenyl tetrazolium bromide (MTT), dimethylformamide (DMF), penicillin and streptomycin, and glutathione assay kit were obtained from Sigma Chemical Co. (St. Louis, MO). 2,7-dichlorofluorescein diacetate (DCF-DA) was purchased from Molecular Probes (Invitrogen Corporation, Carlsbad, CA). Lipid peroxidation assay kit (705002) was purchased from Cayman Chemicals (Ann Arbor, MI). Superoxide dismutase kit was purchased from Trevigen, Inc. Gaithersburg, MD, USA (Cat # 7500-100-K). Coomassie plus protein assay reagent was purchased from Thermo fisher (cat # 1856210).

ZnO Nanorod synthesis

The typical method employed is as follows. Equal volume of 0.1 M aqueous zinc acetate anhydrous and

hexamethylenetetramine were mixed in a beaker using ultrasonication for about 30 min. After the mixture was mixed well, it was heated at 80°C in water bath for 75 min, during which white precipitates were deposited at the bottom. When hexamethylenetetramine was heated, it decomposes into aldehyde and ammonia [18] which produces OH^- ions. Then Zn^{2+} combined with OH^- to form $\text{Zn}(\text{OH})_4^{2-}$ and decomposed into ZnO after heating, as the following formula illustrate:



Then the reaction mixture was incubated for 30 min in ice cold water to terminate the reaction. The product was washed several times (till the pH of solution becomes neutral) using the centrifuge (12,000×g for 20 min) with deionized water and alcohol, alternatively, to remove any by-product and excess of hexamethylenetetramine. Finally, the purified ZnO nanorods were collected and dried at room temperature for 48 h. The resulting white precipitates were used for further characterization. The commercially available ZnO (bulk ZnO from Sigma cat # 96479) was used as the standard for comparison with the prepared ZnO nanorods while characterization.

ZnO Nanorods Characterization

The microscopic characterization of ZnO nanorods were performed using transmission electron microscopy (TEM, JEM-2100, JEOL Instrument, Inc., Japan) and the scanning electron microscopy (SEM, JEOL JSM 5610LV). Nanorods of zinc oxide were suspended in ethanol and exposed to ultrasonic waves. For TEM method, one drop of the suspension was placed on 300 mesh copper grip, which was coated with holey carbon film. Then the sample was dehydrated at 40°C. In case of SEM, the obtained solution was dropped on a carbon tape. Then the sample was dehydrated at 50°C. The structural characterizations were performed using "Rigaku D-max" X-ray diffractometer equipped with Cu K α radiation ($\lambda = 1.5417\text{\AA}$, 40 kV at 40 mA). The structural and molecular composition of nanorods was evaluated by Fourier transform infrared spectroscopy (PerkinElmer, FT-IR system spectrum GX) absorbance spectra. Samples were analyzed using an attenuated total reflectance attachment from 500 cm^{-1} to 4000 cm^{-1} .

Cell Culture and Treatment

Hela Cells (CCL-2) were purchased from American Type Culture Collection (Manassas, VA), cultured in DMEM with 10% FBS, 100 IU/ml of penicillin, and 100 $\mu\text{g}/\text{ml}$ of streptomycin and incubated in a water-saturated atmosphere containing 5% CO_2 at 37°C incubator. For all studies, zinc oxide nanorods stocks (5 mg/ml) were prepared by dissolving in phosphate buffer saline (PBS) pH 7. For control experiments, cells were treated with equivalent volume of PBS.

Detection of Reactive Oxygen Species

The generation of intracellular reactive oxygen species (ROS) was measured using real time assay as described earlier [19]. Briefly, hela cells (1×10^5 cells/well) were seeded in a 96-well plate and grown overnight at 37°C in a humidified chamber with 5% CO₂. The overnight grown cells were then treated with 10 μM of H₂DCF-DA with HBSS and incubation at 37°C for 3 h. Following incubation, cells were washed with PBS and treated with various concentrations of ZnO nanorods. At different time intervals, the intensity of fluorescence was measured at excitation and emission wavelengths of 485/527 nm, respectively, and the values were expressed as fluorescence units.

Cell Viability Assay

The assay for cytotoxicity was performed using MTT, a tetrazole dye, as described earlier [20]. Equal numbers of hela cells (2000 cells/well) were seeded in a 96-well plate and grown overnight at 37°C in a humidified chamber with 5% CO₂. Briefly, following overnight growth, the cells were treated with different concentrations of ZnO nanorods and incubated for 72 h at 37°C. Thereafter, the cells were washed with PBS and MTT was added to a final concentration of 125 μg/ml and incubated for another 3 h at 37°C. The formazans formed inside the cells were extracted using acidic methanol and the absorbance was measured at 570 nm. To reconfirm the cell viability results, a live-dead cell assay was performed essentially as described by Manna et al [19]. Briefly, following treatment with 5 and 10 μg/ml of ZnO nanorods, approximately 10⁵ cells were stained with Live/ Dead reagent (5 μM ethidium homodimer, 5 μM calcein- AM, Molecular Probes, Eugene, OR) and then incubated at 37°C for 30 min. The stained cells were analyzed under fluorescent microscope (Zeiss, Germany).

Lipid Peroxidation Assay

Lipid peroxidation assay was measured using a kit from Cayman Chemicals as described earlier [21]. Equal numbers of hela cells (4×10^5 cells/well) were seeded in a 6-well plate and grown overnight at 37°C in a humidified chamber with 5% CO₂. Following incubation, cells were washed with PBS and treated with 5 and 10 μg/ml of ZnO nanorods and incubated for 24 h at 37°C. The cells were then scraped using PBS, sonicated, centrifuged and followed by protein estimation using coomassie plus protein assay reagent. Fifty micrograms of cell lysate was mixed with equal volume of pre-chilled methanol-chloroform mixture and centrifuged at 1500×g for 10 min. The hydroperoxides presented in the supernatant were collected and used for the estimation of LPO indicator malondialdehyde (MDA). Finally, freshly prepared chromogen was added and absorbance was measured at 500 nm.

Glutathione (GSH) Assay

The concentration of intra cellular GSH was measured as described earlier [22]. In brief, equal numbers of hela cells (4×10^5 cells/well) were seeded in a 6-well plate and grown overnight at 37°C in a humidified chamber with 5% CO₂. The cells were then treated with 5 and 10 μg/ml of ZnO nanorods and incubated for 24 h at 37°C. Then, the cells were scraped and homogenized using PBS. Fifty micrograms of protein was deproteinized using 5% 5-sulfosalicylic acid dihydrate solution and sodium

carbonate (400mM) followed by 1:8 dilutions with phosphate-EDTA buffer and incubated for 10 minutes at room temperature. The supernatant was then treated with 5, 5-di-thiobis (2-nitrobenzoic acid; DTNB) and incubated again at room temperature for 10 min. The GSH activity was measured at 415 nm absorbance.

Total Superoxide Dismutase Assay

Equal numbers of hela cells (4×10^5 cells/well) were seeded in 6-well plates and grown overnight at 37°C in a humidified chamber with 5% CO₂. The cells were then treated with 5 and 10 μg/ml of ZnO nanorods and incubated for 24 h at 37°C. Fifty micrograms of protein extracts were used to assay total SOD activities using the manufacturer's protocol. Briefly, SOD reaction buffer was mixed with xanthine solution followed by NBT solution and then the sample proteins were added and the absorbance was set to zero at 550 nm. Finally, XOD solution was added to each sample and readings were taken at 550 nm every 30 seconds for a period of 5 minutes. The total SOD activity was measured according to manufacturer's instructions.

Results and Discussion

Figure 1 shows the crystalline structure of the synthesized ZnO nanorods measured using XRD. It can be seen that all diffraction peaks are caused by crystalline ZnO with the hexagonal wurtzite structure (space group: $P6_3mc$ (186); $a = 0.3249$ nm, $c = 0.5206$ nm). The data are in agreement with the Joint Committee on Powder Diffraction Standards (JCPDS) card for ZnO (JCPDS 036-1451). No characteristic peaks of impurity phases such as Zn or Zn(OH)₂ were observed. Also, no diffraction peaks except ZnO were found. As seen in Fig. 1, the strongest detected ($h k l$) peaks are at $2\theta^\circ$ values of 31.7°, 34.4°, 36.2°, 47.5° and 56.6° corresponding to the following lattice planes: (100), (002), (101), (102), and (110) respectively. The XRD pattern indicates a (002)-preferred orientation, which suggests that the rods are quasi-aligned with the optical c -axis which is oriented perpendicularly to the substrate surface.

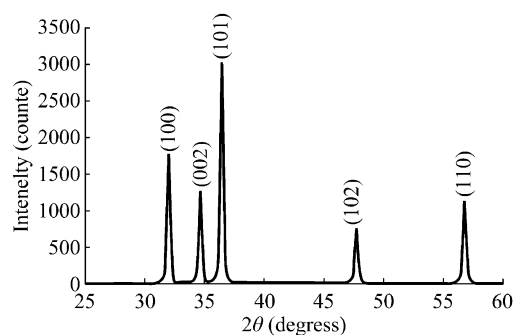


FIG. 1. X-ray diffraction patterns of ZnO nanorods.

Figure 2 (a&b) shows the SEM micrograph collected on synthesized ZnO nanorods surface morphology. The nanorod was grown perpendicular to the long-axis of the matrix rod and grew along the [001] direction, which is the nature of ZnO growth. The morphology of ZnO from the individual crystalline nucleus, was further confirmed by the TEM image as shown in Fig. 2 (c&d). A similar morphology of ZnO was previously observed by [23]. Though the rod cores were monodisperse, the

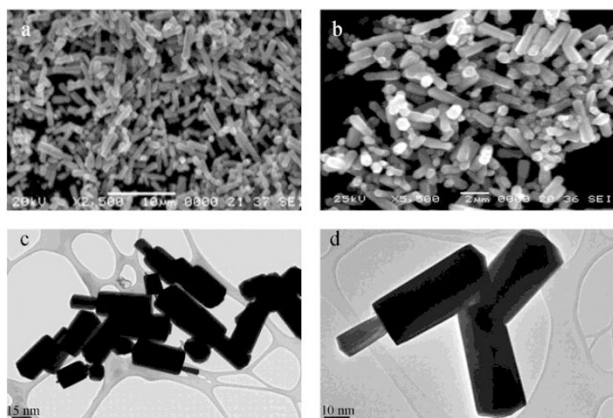


FIG. 2. (a&b) Scanning electron micrograph of ZnO nanorods. (c&d) Transmission electron micrograph of ZnO nanorods.

length of the nanorod was estimated to be around 21 nm in diameter and the length around 50 nm.

Figure 3 illustrates the FTIR spectra of the synthesized ZnO nanorods with hexamethylenetetramine at room temperature. The characteristic absorbances were collected in the IR range from 4000 to 400 cm^{-1} . A peak at 418 cm^{-1} is the stretching vibration of the Zn-O bond in ZnO particles. The peaks at 2857 cm^{-1} are assigned to the vibration of the C-H bond of the precursor. A broad absorption band at 3423 cm^{-1} in the IR spectra of ZnO particles can be seen, and these are attributed to the hydroxyl groups. Because the samples were immersed in the water during the growth of ZnO nanorods, the oxygen adsorbed to the surface would rather become O-H.

The production of free radicals has been found in a diverse range of nanomaterials which is one of the primary mechanisms of NPs toxicity [2]. Oxidative stress is caused by an imbalance in the level of reactive oxygen and a biological system's ability to readily detoxify the reactive intermediates. Increased level of oxidative damage causes a net stress on the normal body functions, leading to a gradual loss of vital physiological functions. In order to check our synthesized ZnO nanorods for its biocompatibility, we used hela cells; an immortalized cervical cancer cells. Hela cells were treated with different concentration (0.5, 1.0, 2.0, 2.5, 5.0, 10 $\mu\text{g}/\text{ml}$) of ZnO nanorods for 3 h. They showed no significant induction of ROS (see Fig. 4a). Our earlier

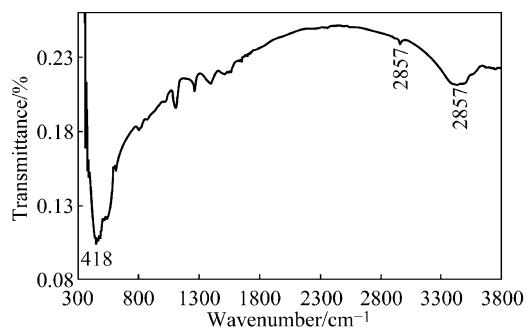
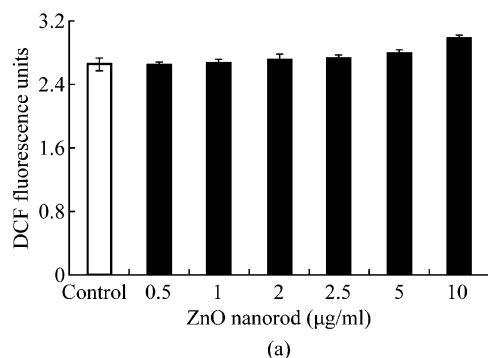


FIG. 3. FT-IR spectra for ZnO nanorods .

studies using different nanoparticles such as single and multi walled carbon nanotubes showed significantly increased levels of ROS at 5-10 $\mu\text{g}/\text{ml}$. [19-22], whereas, here in ZnO nanorods, we did not detect any increase in ROS level even in 20 $\mu\text{g}/\text{ml}$ (data not shown). The time kinetics was also performed to check the formation of ROS (see Fig. 4b). Our data show that, there is no significant ROS level formed as early as 30 min with 10 $\mu\text{g}/\text{ml}$ of ZnO nanorods and remained same till 150 min. However, at later time intervals the increase in ROS was observed in 10 $\mu\text{g}/\text{ml}$ but very less as compared to the control. This may be due to osmotic pressure created by excess of nanorods. Next, we investigated the level of lipid peroxidation in ZnO nanorods exposed hela cells; another possible player for oxidative stress induction. As shown in Fig. 5, we observed very minimal (as low as 0.1 fold) increase in lipid peroxidation level with 10 $\mu\text{g}/\text{ml}$ of ZnO nanorods as compared to the control.

In order to check whether ZnO nanorod has any role on toxicity without altering oxidative stress, we extended our studies by analyzing cell damage using MTT assay after exposing to various concentration of ZnO nanorods (0.5, 1.0, 2, 2.5, 5.0, 10 $\mu\text{g}/\text{ml}$) (see Fig. 6a). The MTT assay showed no significant decrease in cell viability suggesting that ZnO nanorods did not have any effect on cell toxicity. We observed that more than 98% of cells were viable at concentration of 10 $\mu\text{g}/\text{ml}$ ZnO nanorods which is also confirmed by live dead cell assay (see Fig. 6b). Fifty percentage of cell death was observed in mouse neuroblastoma cells using 100 $\mu\text{g}/\text{ml}$ of ZnO [24], whereas other reports have also shown 100% cytotoxicity at 15 $\mu\text{g}/\text{ml}$ of ZnO on mesothelioma MSTO-211H or rodent 3T3

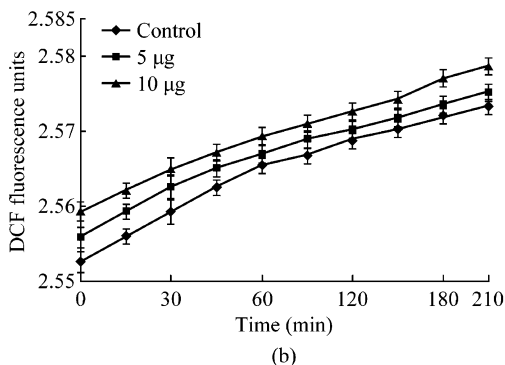


FIG. 4. Effect of ZnO nanorods on oxidative stress. Equal numbers of 1×10^5 hela cells/well were grown for 18 h. (a) The grown cells were incubated with 10 μM of DCF for 3 h, treated with different concentration of ZnO nanorods. Fluorescence was measured at excitation and emission wavelengths of 485 and 527 nm, respectively, at the end of 3 h. (b) Time kinetics of ROS formation by ZnO nanorods. Overnight grown hela cells were treated with 1, 5, and 10 $\mu\text{g}/\text{ml}$ of ZnO nanorods. Fluorescence was measured at excitation and emission wavelengths of 485 and 527 nm, respectively, at different time points. The values are expressed as DCF fluorescence units, mean \pm SD of eight wells and the figure is a representative of three experiments performed independently.

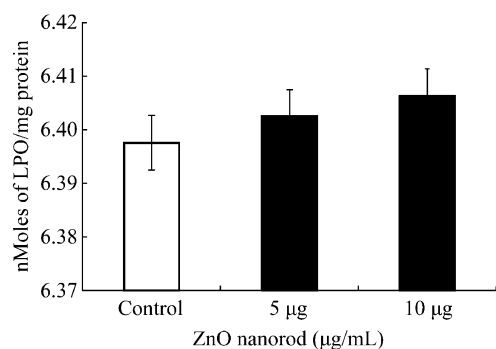


FIG. 5. Effect of ZnO nanorods on lipid peroxidation: 4×10^5 hela cells were grown for 24 h. Cells were then treated with 5 and 10 µg/ml of ZnO nanorods and allowed to grow for 24 h at 37°C. Lipid peroxidation levels were measured from chloroform-methanol extracts. Values are mean \pm SD of three independent experiments.

fibroblast cells [25], and 90% cell death with 20 mgL⁻¹ of ZnO nanoparticles on HELF cells [26]. Also, 5 mM of ZnO nanoparticle are shown to be less toxic to human T cells [27]. Previous studies from our laboratory on hela cells and other cells such as lung epithelial, H1299, A549 and HaCaT cells showed the decrease in cell viability at 5 µg/ml when they were exposed to SWCNT and MWCNT [19-22].

During normal conditions, important antioxidant enzymes Glutathione (GSH), along with superoxide dismutase SOD are effective in scavenging free radicals [20]. Therefore in this study, the effect of ZnO nanorods on levels of antioxidants, GSH and SOD assays were performed. GSH is a ubiquitous sulfhydryl containing molecule in cells that is responsible for maintaining cellular oxidation-reduction homeostasis [28]. Hela cells treated with 5 and 10 µg/ml of ZnO nanorods for 24 h were used to analyze GSH and SOD levels (see Fig. 7 a&b) and showed no significant decreasing level of total GSH and SOD levels even at high concentration of 10 µg/ml.

Conclusion

In this study, we have synthesized ZnO nanorods by mixing zinc acetate and hexamethylenetetramine and characterized using X-ray diffraction, scanning electron microscopy, high resolution transmission electron microscopy, and fourier transform infrared spectroscopy. XRD measurements indicate that the synthesized nanorods are in the hexagonal wurtzite structure with high crystallinity and preferred growth direction

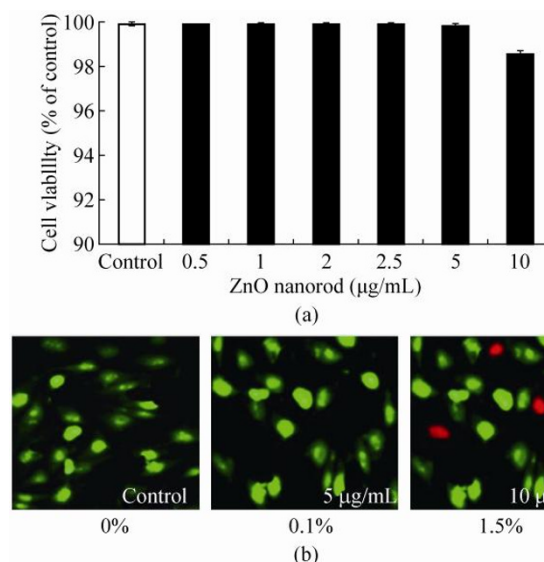
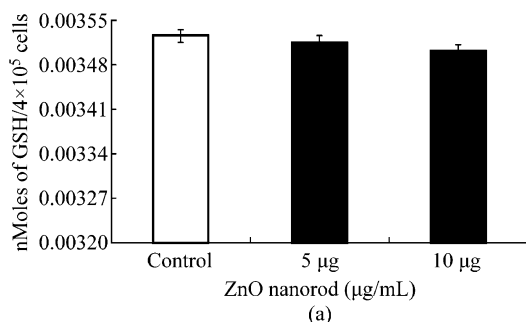


FIG. 6. Effect of ZnO nanorods on cell viability. HeLa cells (2000/well in a 96-well plate) were incubated for 12 h and treated with different concentration of ZnO nanorods for 72 h. (a) Cell viability was assayed by MTT dye uptake. The mean absorbance at 570 nm is represented as cell viability percentage of the control and is mean \pm SD of eight wells. (b) HeLa cells were treated with 5 µg/ml and 10 µg/ml of ZnO nanorods for 72 h and the dead cell (red color) numbers were counted. The percentage of dead cells is indicated below each photograph.

of the c-axis. The length of the nanorods estimated by TEM and XRD is around 21 nm in diameter and 50 nm in length. FT-IR characterization confirmed the presence of nanorods. In addition, our toxicological studies using synthesized ZnO nanorods on hela cells showed no significant induction of oxidative stress and cell death even at high concentration of 10 µg/ml. In summary, we report here the successful preparation of ZnO nanorods, characterization and toxicological studies on hela cells and conclude that ZnO nanorods could be the safe nanomaterial for biological applications.

This work was supported by NASA funding NNX08BA47A, NCC-1-02038, NIH-1P20MD001822-1, NSF (RISE) HRD-0734846.

Received 3 March 2010; accepted 16 March 2010; published online 23 March 2010.

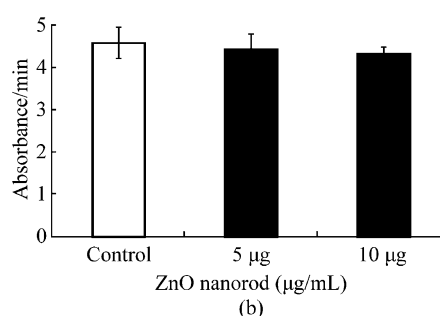


FIG. 7. Effect of ZnO nanorods on antioxidants level. Equal numbers of 4×10^5 hela cells/well were grown for 24 h and treated with 5 and 10 µg/mL of ZnO nanorods and allowed to grow for additional 24 h. a) Total GSH was measured at 412 nm and the values were expressed in nanomoles. b) Superoxide dismutase activity was assayed from each sample and activity was measured at 550 nm. Values are mean \pm SD of three experiments performed independently.

References

1. S. E. McNeil and J. Leuk. *Bio.* 78, 585 (2005).
2. A. Nel, T. Xia, L. Madler and N. Li, *Science* 311, 622 (2006). [doi:10.1126/science.1114397](https://doi.org/10.1126/science.1114397)
3. D. A. Groneberg, M. Giersig, T. Welte and U. Pison, *Curr. Drug Targets.* 7, 643 (2006). [doi:10.2174/138945006777435245](https://doi.org/10.2174/138945006777435245)
4. D. M. Balshaw, M. Philbert and W. A. Suk, *Toxicol. Sci.* 88, 298 (2005). [doi:10.1093/toxsci/kfi312](https://doi.org/10.1093/toxsci/kfi312)
5. Y. Lee, D. S. Ruby, D. W. Peters, B. B. McKenzie and J. P. Hsu, *Nano Lett.* 8, 1501 (2008). [doi:10.1021/nl080659j](https://doi.org/10.1021/nl080659j)
6. T. Thomas, K. Thomas, N. Sadrieh, N. Savage, P. Adair and R. Bronaugh, *Toxicol. Sci.* 91, 14 (2006). [doi:10.1093/toxsci/kfj129](https://doi.org/10.1093/toxsci/kfj129)
7. T. Ma, M. Guo, M. Zhang, Y. Zhang and X. Wang, *Nanotech.* 18, 035605 (2007). [doi:10.1088/0957-4484/18/3/035605](https://doi.org/10.1088/0957-4484/18/3/035605)
8. U. O. Zgur, Y. I. Alivov, C. Liu, A. Teke, M. A. Reshchikov, S. Dogan, V. Avrutin, S. J. Cho and H. Morkoc, *J. Appl. Phys.* 98, 041301 (2005).
9. T. Ghoshal, S. Kar and S. Chaudhuri, *J. Cryst. Growth* 293, 438 (2006). [doi:10.1016/j.jcrysgro.2006.06.002](https://doi.org/10.1016/j.jcrysgro.2006.06.002)
10. H. Yang, C. Liu, Hui, D. Yang, H. Zhang and Z. Xi, *J. Appl. Toxicol.* 29, 69 (2009). [doi:10.1002/jat.1385](https://doi.org/10.1002/jat.1385)
11. X. Y. Deng, Q. X. Luan, W. T. Chen, Y. L. Wang, M. H. Wu, H. J. Zhang and Z. Jiao, *Nanotechnology* 20, 115101 (2009). [doi:10.1088/0957-4484/20/11/115101](https://doi.org/10.1088/0957-4484/20/11/115101)
12. D. H. Lin and B. S. Xing, *Environ. Pollut.* 150, 243 (2007). [doi:10.1016/j.envpol.2007.01.016](https://doi.org/10.1016/j.envpol.2007.01.016)
13. L. K. Adams, D. Y. Lyon and P. J. Alvarez, *Water Res.* 40, 3527 (2006). [doi:10.1016/j.watres.2006.08.004](https://doi.org/10.1016/j.watres.2006.08.004)
14. J. M. Fine, T. Gordon, L. C. Chen, P. Kinney, G. Falcone and W. S. Beckett, *J. Occup. Environ. Med.* 39, 722 (1997). [doi:10.1097/00043764-199708000-00006](https://doi.org/10.1097/00043764-199708000-00006)
15. W. S. Beckett, D. F. Chalupa, A. Pauly-Brown, D. M. Speers, D. J. Stewart, M. W. Frampton, D. J. Utell, L. S. Huang, C. Cox, W. Zareba and G. Oberdorster, *Am. J. Respir. Crit. Care Med.* 171, 1129 (2005). [doi:10.1164/rccm.200406-837OC](https://doi.org/10.1164/rccm.200406-837OC)
16. X. Hu, S. Cook, P. Wang and H. Hwang, *Sci. Total Environ.* 407, 3070 (2009). [doi:10.1016/j.scitotenv.2009.01.033](https://doi.org/10.1016/j.scitotenv.2009.01.033)
17. T. Zaveri, N. Dolgova, B. H. Chu, J. Lee, T. Lele, F. Ren and B. G. Keselowsky, *IFMBE Proceedings*. Springer, Berlin, Heidelberg 24, 119 (2009).
18. J. G. Strom, H. W. Jun and J. Pharm. Sci. 69, 1261 (1980). [doi:10.1002/jps.2600691107](https://doi.org/10.1002/jps.2600691107)
19. S. Sarkar, C. Sharma, R. Yog, A. Periakaruppan, O. Jejelowo, R. Thomas, E. V. Barrer, A. C. Rice-Ficht, B. L. Wilson, G. T. Ramesh and J. Nanosci, *Nanotechnology* 7, 584 (2007).
20. S. K. Manna, S. Sarkar, J. Barr, K. Wise, E. V. Barrera, O. Jejelowo, A. C. Rice-Ficht and G. T. Ramesh, *Nano Lett.* 5, 1676 (2005). [doi:10.1021/nl0507966](https://doi.org/10.1021/nl0507966)
21. C. S. Sharma, S. Sarkar, A. Periyakaruppan, J. Barr, K. Wise, R. Thomas, B. L. Wilson and G. T. Ramesh, *J. Nanosci. Nanotechnology* 7, 2466 (2007).
22. P. Ravichandran, A. Periyakaruppan, B. Sadanandan, V. Ramesh, J. C. Hall, O. Jejelowo and G. T. Ramesh, *J. Biochem. Mol. Tox.* 23, 333 (2009). [doi:10.1002/jbt.20296](https://doi.org/10.1002/jbt.20296)
23. J. Tang and X. Yang, *Mat. Lett.* 60, 3487 (2006). [doi:10.1016/j.matlet.2006.03.037](https://doi.org/10.1016/j.matlet.2006.03.037)
24. V. Prasad, C. D. Souza, D. Yadav, A. J. Shaikh and N. Vigneshwaran, *Spectrochim. Acta* 65, 173 (2006). [doi:10.1016/j.saa.2005.10.001](https://doi.org/10.1016/j.saa.2005.10.001)
25. T. J. Brunner, P. Wick, P. Manser, P. Spohn, P. N. Grass, L. Limbach, A. Bruinink and W. J. Stark, *Environ. Sci. Tech.* 40, 4374 (2006). [doi:10.1021/es052069j](https://doi.org/10.1021/es052069j)
26. J. H. Yuan, Y. Chen, H. X. Zha, L. J. Song, C. Y. Li, J. Q. Li and X. H. Xia, *Colloids and Surfaces B: Biointerfaces* 76, 145 (2010). [doi:10.1016/j.colsurfb.2009.10.028](https://doi.org/10.1016/j.colsurfb.2009.10.028)
27. K. M. Reddy, K. Feris, J. Bell, D. J. Wingett, C. Hanley and A. Punnoose, *Appl. Phys. Lett.* 90, 213902 (2007). [doi:10.1063/1.2742324](https://doi.org/10.1063/1.2742324)
28. H. Sies, *Free. Radic. Biol. Med.* 27, 916 (1999). [doi:10.1016/S0891-5849\(99\)00177-X](https://doi.org/10.1016/S0891-5849(99)00177-X)